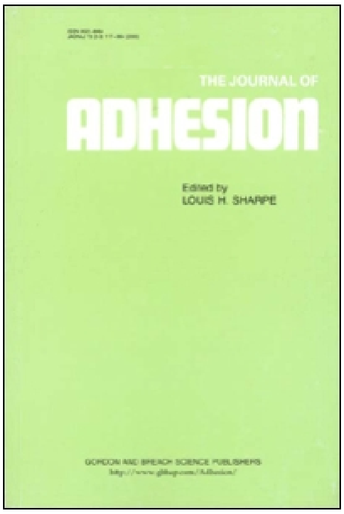

The Journal of Adhesion
Publication details, including instructions for authors and subscription information:
http://www.informaworld.com/smpp/title~content=t713453635

The Effect of Lateral Constraint on the Strength of a Single Lap Joint

I. D. Steg[a]; O. Ishai[a]
[a] Faculty of Mechanical Engineering, Technion-Israel Institute of Technology, Haifa, Israel

To cite this Article Steg, I. D. and Ishai, O.(1977) 'The Effect of Lateral Constraint on the Strength of a Single Lap Joint', The Journal of Adhesion, 8: 4, 263 — 273
To link to this Article: DOI: 10.1080/00218467708075089
URL: http://dx.doi.org/10.1080/00218467708075089

J. Adhesion, 1977, Vol. 8, pp. 263–273

The Effect of Lateral Constraint on the Strength of a Single Lap Joint

I. D. STEG and O. ISHAI

Faculty of Mechanical Engineering, Technion-Israel Institute of Technology, Haifa, Israel 32000

(*Received April 9, 1976*)

The mechanical performance of a single lap joint (SLJ) is mainly affected by the lateral normal tensile stresses acting at the edges of its interlaminar adhesive layer (IAL). Owing to these stresses, the delamination failure which initiates at the IAL edges and propagates inward, is predominantly of the peel type. The subject of this study is the effect of constraint of the lateral deflection of adhering edges applied by tightly binding them together.

Experimental results showed that the effect of this type of constraint is a reduction in the extent of peel and an overall increase in the joint tensile strength. This effect is more pronounced in the case of brittle than in the case of ductile adhesives.

INTRODUCTION

A relatively hard, brittle adhesive, such as an epoxy resin, may give a highly satisfactory performance in a joint designed for shear stresses with negligible peel components,[1] but in the presence of peel stress its performance may be very poor. This effect may be demonstrated in the case of the single lap joint (SLJ).

Because of its simplicity, SLJ testing has been selected as a standard industrial method for the evaluation of the adhesion performance. However, mechanical interpretation of the experimental data obtained in the test is difficult, and often fails to reflect the expected performance of the structural bonded joint. Most studies of the stress analysis of SLJ are based on the classical work of Goland and Reissner,[2] which is limited to the relatively simple case of adherends having equal thickness and identical material properties. The results indicate the presence of high interlaminar peel and shear stresses at the edges of the overlap bond-line, which are directly related to the applied external load.† The weak link in most bonded joints is located at the adherend–adhesive interface. In such cases, the bond failure originates at the end of the interfacial zone and propagates inwards along the bondline. Such brittle-like delamination is mainly governed by the peel stresses acting on the adhesive layer in the direction perpendicular to the bondline axis.

Peel stress effects may be reduced by using a tougher, high-peel adhesive; another solution, which is discussed in the present paper, is to apply external lateral constraints.

An analysis of an analog model, with a mechanical behavior similar to that of SLJ,[4] indicates that such a lateral constraint, if applied at the edges of the joint, would not affect interlaminar shear stresses significantly. This study is an attempt to examine the effect of such a constraint on the ultimate strength of the SLJ which is determined by the combined effects of interlaminar peel and shear stresses.

EXPERIMENTAL

Specimens of aluminum 2024, 105 × 12.5 × 1.5 mm, were used to prepare single lap joints in a specially designed device (see Figure 3).

Materials employed

1) *Epoxy resin* E-826a, manufactured by Shell Co., purchased from Miller and Stephenson, Danbury, Conn., U.S.A. This product was chosen because it is an almost pure chemical compound (practically pure diglycidyl-ether of bisphenol-A) (DGBA) and because of its relatively low viscosity.

2) Epon-Z curing agent, manufactured by Shell Co., purchased from Miller and Stephenson, Danbury, Conn., U.S.A.

3) Thiokol LP-8, flexibilizer, a product of Thiokol Chem. Corp., Trenton, N.J., U.S.A.

The curing agent and the flexibilizer were added to the epoxy resin in the amounts of 20 and 10 PHR (parts per hundred of resin) respectively.

Curing technique

The joints were placed in the device and then in the curing oven. They were then cured for 3 hours at 75°C, followed by 4 hours at 120°C, and were then slowly cooled to room temperature.

† Though Goland and Reissner's solution violates equilibrium conditions at the adhesives edge, the stress distribution at a region close to the edges is in agreement with more recent solutions obtained by finite element methods.[3]

Winding of glass reinforced plastic (GRP) lateral constraints

In order to ensure the homogeneity of the compressive external stress, semi-cylindrical aluminum pieces were glued onto the outer face of the SLJ with the aid of a paper glued on both sides before the winding began. This assembly was sprayed with Ram release agent in order to prevent the resin *from penetrating to SLJ surfaces* during the winding.

The winding of "FRP constraints" was performed by using a simple winding machine, the SLJ serving as mandrel, as shown in Figure 4.

The wet wound SLJ were placed in an oven and the curing procedure described above was repeated.

The following series of wound and non-wound SLJ were prepared. Of these, the first six series had a bond line thickness of 0.08–0.12 mm. In order to examine the effect of compression stresses induced by the winding, a preliminary series of 5 wound specimens (1.5 cm overlap) without adhesive were prepared and tested. Results show negligible strengthening effect (Table I).

1) E-826/Z—1.5; 3; 5; 7 cm overlap length nonwound
2) E-826/Z/LP-3—1.5; 3; 5; 7 cm overlap length nonwound
3) E-826/Z—1.5; 3; 5; 7 cm and 0.5 cm wound on both ends
4) E-826/Z—1.5; 3; 5; 7 cm whole overlap length wound
5) E-826/Z/LP-3—1.5; 3; 5; 7 cm and 0.5 cm wound on both ends
6) E-826/Z/LP-1.5—3; 3; 5; 7 cm whole overlap length wound

Experimental results

The prepared SLJ were loaded in tension by an Instron tester at a rate of 0.2 cm/min, in accordance with the ASTM-1002 method. Results are shown in Table I and Figure 1. It is seen that:

a) Lateral constraint of specimens with SLJ made of brittle epoxy adhesive by means of wound GRP rings results in a more than 140% increase in the strength of the joint.

b) A more flexible adhesive yields a much stronger joint than a brittle adhesive.

c) As could have been expected, there is no major difference (about 20%) between joints given by flexible and brittle adhesives, if the joints are constrained.

d) Similar values of joint strength were obtained for both partially wound and whole-length-wound constraining GRP rings.

e) The constrained, nonglued SLJ had a marginal (7–10 kg/cm²) shear strength.

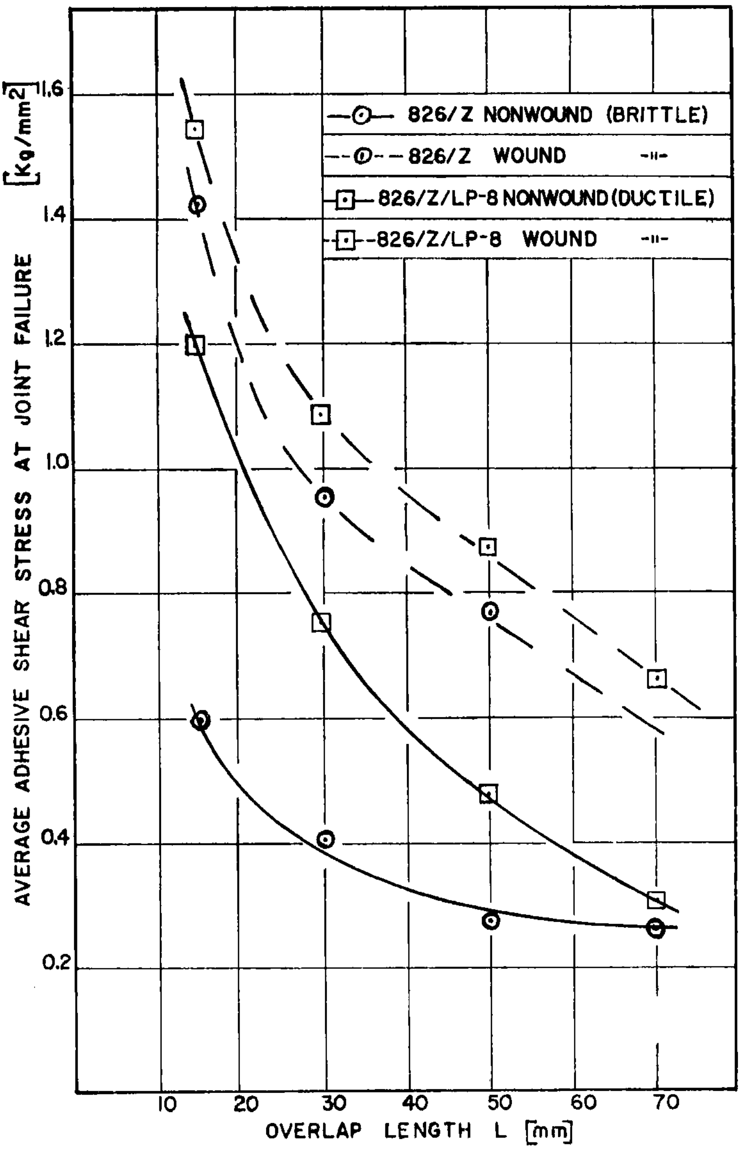

FIGURE 1 Average adhesive shear stress (τ) at joint failure as a function of overlap length (l) in constrained and unconstrained joints made with brittle and ductile epoxy adhesives.

TABLE I

Experimental data

Composition	Average shear stress τ (kg/cm^2)	Overlap length l [cm]	Width of the lateral winding [cm]	Remarks
E-826/Z	145	1.5	1.5	1. The shear stress figures represent an average of 6 experiments.
E-826/Z	60	1.5	0	
E-826/Z/LP-8	118	1.5	0	
E-826/Z/LP-8	162	1.5	1.5	
Without adhesive	8	1.5	1.5	2. 1+①+1 means that the middle part (1 cm) of the SLJ remained non-wound.
E-826/Z	114	3.0	1+①+1	
E-826/Z	113	3.0	3	3. E-826/Z brittle adhesive.
E-826/Z	45	3.0	0	4. E-826/Z/LP-8 ductile adhesive.
E-826/Z/LP-8	76	3.0	0	
E-826/Z/LP-8	120	3.0	3	5. The bondline thickness in all SLJ was 0.08–1i12 mm.
E-826/Z	40	5.0	0	
E-826/Z/LP-8	69	5.0	5	
E-826/Z/LP-8	70	5.0	0.5+④+0.5	
E-826/Z/LP-8	51	5.0	0	
E-826/Z	30	7.0	0	
E-826/Z/LP-8	56	7.0	1+⑤+1	

ANALYTICAL

Several elastic solutions for shear and peel stress distributions along the adhesive bond line have been proposed.[2-8]. The capability of the various strength theories to predict the values of the ultimate load on the bond was much less intensively studied partly due to the lack of failure envelopes for the adhesive layer *in situ*.

An attempt of such an analysis which permits an approximate, comparative prediction of single-lap joint performance is presented here. The analysis is based on the classical theories of strength of isotropic materials. The following assumptions will be made:

a) It will be assumed that the adhesive displays a linear-elastic behavior up to the point of fracture or yield initiation. Other assumptions and expressions given in Ref. 2 and 5 will also be assumed to be valid.

b) The two modes of failure being compared are the predominantly brittle and ductile ones. In the former case it is assumed that interfacial adhesive failure occurs mainly due to the interlaminar peel stress component. For the ductile case, it is assumed that a combination of interlaminar shear (τ_y) and peel (σ_y) stresses is responsible for "cohesive" failure, in accordance with von Mises's energy criterion.

c) Initiation of failure of adhesive layer occurs close to the interlaminar edges where shear and peel stress components assume their maximum values.

d) It is assumed[4] that in the case of external lateral constraint applied along the overlap length, interlaminar peel stresses are negligible and the shear stresses in the adhesive are unaffected by the constraint. The states of stress at the adhesive layer edges and the relevant strength criteria for the "ductile" and "brittle" cases are illustrated in Table II.

TABLE II

States of stress of adhesive layer edges for "ductile" and "brittle" cases

	"Ductile" adhesive	"Brittle" adhesive
Unconstrained		
Strength criterion	$\sigma_0^2+3\tau_0^2 = \sigma_{ay}^2$	$\sigma_0 = \sigma_{iu}$
Constrained		
Strength criterion	$3\tau_c^2 = \sigma_{ay}^2$	$\tau_c = \tau_{au}$

Here σ_0, τ_0, σ_c, τ_c are the maximum peel and shear stresses acting at the adhesive edges in cases of non-constrained and constrained boundary conditions respectively; σ_{ay} and τ_{au} are the tensile yield and the ultimate shear stresses of the ductile and brittle adhesive respectively; σ_{iu} is the interfacial adhesive-adherend ultimate tensile stress, and $\bar{\sigma}_0$ and $\bar{\sigma}_c$ are the average stresses applied to the adherend with free and constrained edges respectively.

The ductile adhesive

An approximate linear relationship may be assumed[2, 5] for the dependence of maximum adhesive stresses on the applied external stress $\bar{\sigma}_0$. Thus for the unconstrained case:

$$\tau_0 = \alpha_0\bar{\sigma}_{0u} \tag{1}$$

$$\sigma_0 = \beta_0\bar{\sigma}_{0u} \tag{2}$$

while for the constrained case

$$\tau_c = \alpha_c \bar{\sigma}_c \simeq \alpha_c \bar{\sigma}_c \tag{3}$$

According to Ref. 4 it is reasonable to assume that $\alpha_0 \simeq \alpha_c$, where α_0, β_0, α_c, are stress-independent functions.

Introducing von Mises's ductile strength criterion for the unconstrained case:

$$\sigma_{ay}^2 = \sigma_0^2 + 3\tau_0^2 = (\beta_0^2 + 3\alpha_0^2)\bar{\sigma}_{0u} \tag{4}$$

and for the constrained case:

$$\sigma_{ay}^2 = 3\tau_c^2 = 3\alpha_0^2 \bar{\sigma}_{cu}^2 \tag{5}$$

Equating (4) and (5):

$$\frac{\bar{\sigma}_{cu}^2}{\sigma_{0u}^2} = \frac{\beta_0^2 + 3\alpha_0^2}{3\alpha_0^2} = 1 + \frac{\beta_0^2}{3\alpha_0^2} \tag{6}$$

and

$$\eta_d = \left[1 + \frac{\beta_0^2}{3\alpha_0^2}\right]^{\frac{1}{2}} \tag{7}$$

η_d is the so-dalled constraint-strengthening factor for ductile adhesives. $\bar{\sigma}_{0u}$ and $\bar{\sigma}_{cu}$ are the joint strength values for the free and constrained cases respectively.

The brittle adhesive

Introducing maximum stress criterion for the brittle case and using Eqs. (2) and (3), we obtain

$$\sigma_{iu} = \sigma_0 = \beta_0 \, \bar{\sigma}_{0u} \quad \text{for free edges, and} \tag{8}$$

$$\tau_{au} = \tau_c = \alpha_0 \, \bar{\sigma}_{cu} \quad \text{for the constrained case.} \tag{9}$$

This yields:

$$\frac{\bar{\sigma}_{cu}}{\bar{\sigma}_{0u}} = \frac{\beta_0}{\alpha_0} \frac{\tau_{au}}{\sigma_{iu}} = \eta_B \tag{10}$$

η_B is the so-called constraint-strengthening factor for the brittle adhesive. For the derivation of α_0 and β_0, which are functions of the geometrical and material parameters of the joints, see Ref. 2 and the Appendix.

DISCUSSION

Parameters α_0 and β_0 were calculated from the experimental parameters given in Table III for the joints studied. The strengthening factors for the brittle and ductile adhesives were calculated using Eqs. (7) and (10), and are

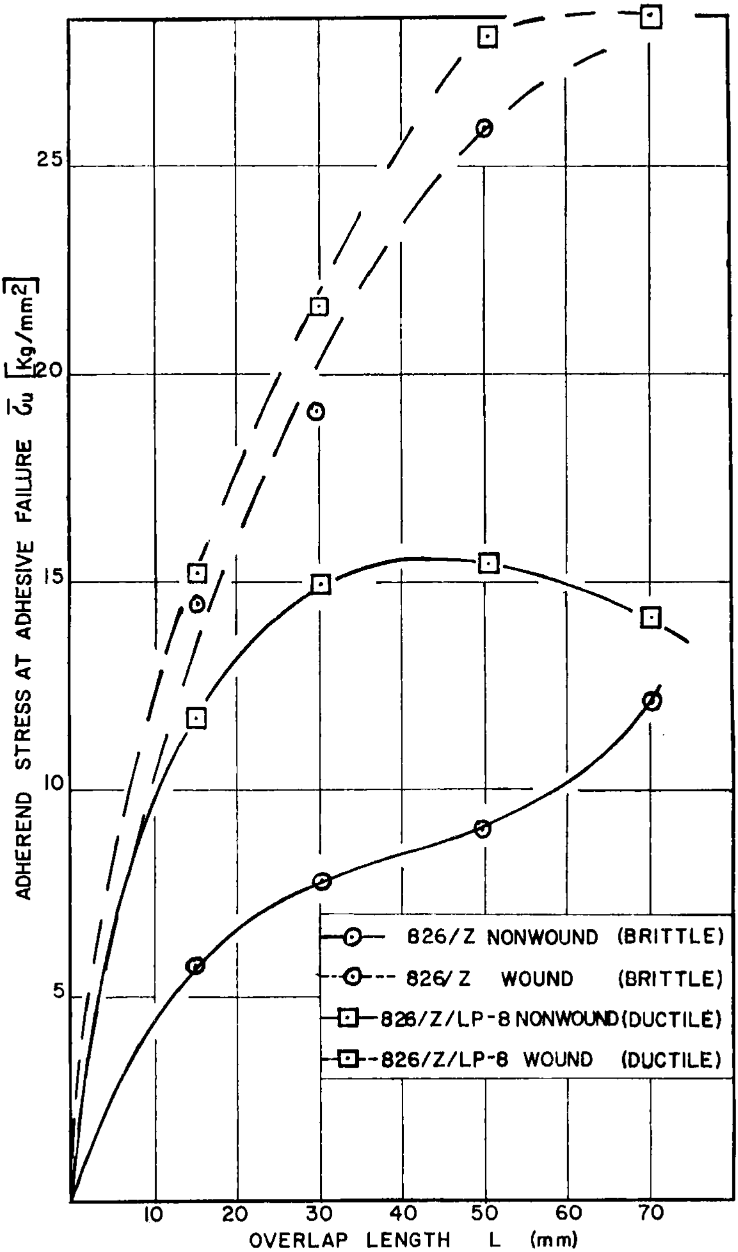

FIGURE 2 Adherend stress ($\bar{\sigma}_u$) at adhesive failure as a function of overlap length (*l*) in constrained and unconstrained joints made with brittle and ductile epoxy adhesives.

compared in Table IV with the experimental values of adherend stresses at joint failure, taken from Figure 2.

TABLE III

Material and geometrical parameters of single-lap joint (for 2C = 15 mm) components

	Dimensions [mm]			Elastic moduli [kg/mm²]			Strength parameters [kg/mm²]		
	C	h_0	h	E	G_0	E_0	σ_{ay}	τ_{au}	σ_{iu}
Brittle case	7.5	0.08	1.5	7500	130	350	—	3.5	1.8
Ductile case	7.5	0.08	1.5	7500	85	240	4.5	—	—

A good agreement between the experimental findings and analytical predictions for the constraint strengthening effect is evident. However, it must be noted that the values of interfacial adhesive strength σ_{iu} and τ_{au} are difficult to determine directly, and they display a high scatter and sensitivity. Thus, only the qualitative analytical trends could be confirmed experimentally.

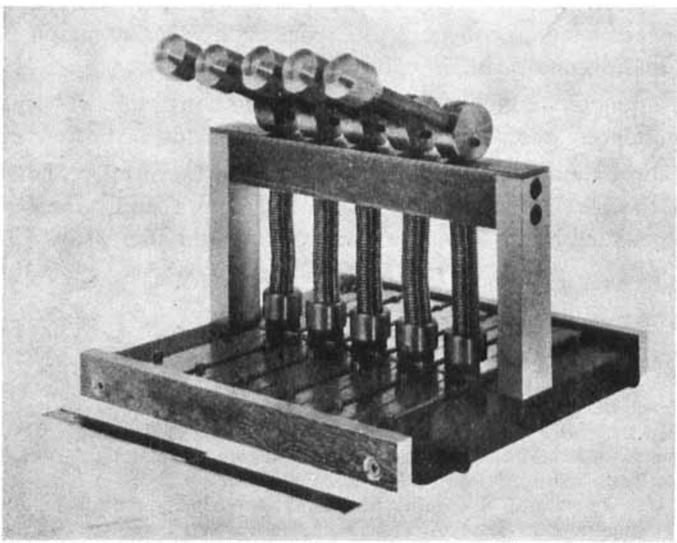

FIGURE 3 A photograph of SLJ preparation device.

TABLE IV

Strength data for SLJ ($2c = 15$ mm)

	SLJ strength [kg/mm²]		Parameters		Constrained strengthening factor	
	$\bar{\sigma}_{ou}$	$\bar{\sigma}_{cu}$	α_0	β_0	$\eta_{experim.}$	$\eta_{theoretical}$
Brittle case	5.8	14.2	0.50	0.56	2.45	2.17
Ductile case	12.0	15.2	0.61	0.63	1.27	1.17

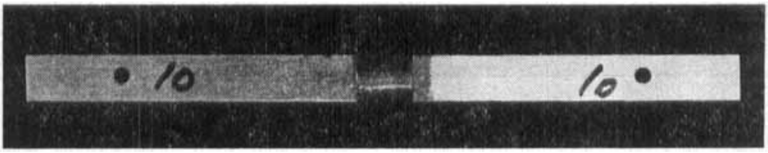

FIGURE 4 A photograph of a GRP ring constrained single lap joint.

CONCLUSIONS

1) It has been experimentally shown that much higher joint strengths are obtained when a lateral constraint is applied to the overlap region of a single lap joint than when no such constraint is present.

2) The strengthening effect produced by the constraint was significantly more pronounced when brittle rather than ductile adhesives were employed.

3) An approximate analytical study of the constraint effect, based on the available theories for bond-line stress distribution and adhesives failure criteria, predicted trends similar to the experimental findings.

References

1. J. J. Bikerman, *The Science of Adhesive Joints* (Academic Press, N.Y., 1961). Chap. 7, p. 163.
2. M. Goland and E. Reissner, *J. Applied Mech.* **11**, 17 (1944).
3. J. N. Dickson *et al.*, "Development of an understanding of the fatigue phenomena of bonded and bolted joints in advanced filamentary composite materials", Vol. 1, Analysis Methods. Technical Report AFFDL-TR-72-64 (1972).
4. O. Ishai, D. Peretz and N. Galili, "Mechanical behavior of multimaterial composite systems—interlaminar behavior", Final Technical Report, TDM 75-5, Technion-I.I.T., U.S. Army Contract No. DAJA-37-74-C-2531, January (1975).
5. E. W. Kuenzi and G. H. Stevens, "Determination of the mechanical properties of adhesives for use in the design of bonded joints", U.S.-FPL Report FPL-011 (1963).

6. R. W. Cornell, *J. of Applied Mechanics* **20,** 355 (1953).
7. O. Volkerson, *Construction Metalliane* **4,** 3 (1965).
8. L. J. Hart-Smith, "Adhesive-bonded single-lap joints", NASA Contract, Report No. NASA-CR-112236 (1973).
9. W. J. Renton and J. R. Vinson, "The analysis and design of composite material bonded joints", Report No. 1, AFOSR-TR-73-1627 (1973); Report No. 2, AFOSR-TR-75-0125 (1974).

APPENDIX

Formulations for parameters α_0 and β_0 as defined in Eqs. (1) and (2)

$$\alpha_0 \simeq \frac{h}{c}\frac{1}{8}\left[\frac{\delta c}{h}(1+3K)+3(1-K)\right] \tag{11}$$

$$\beta_0 = \frac{h^2}{c^2}\left[\lambda^2\frac{K}{2}-\lambda K'\right] \tag{12}$$

assuming $c/h < 4$

$$\delta = \left[\frac{8G_0 h}{Eh_0}\right]^{\frac{1}{2}} \tag{13}$$

$$\lambda = \frac{\gamma c}{h} \tag{14}$$

$$K = \frac{1}{1+2\sqrt{2}\tanh(m\xi)} \tag{15}$$

$$K' = \sqrt{2}m\xi K \tag{16}$$

$$m = \left[\frac{3(1-\nu^2)}{2}\right]^{\frac{1}{2}} \tag{17}$$

$$\xi = \frac{c}{h}\left[\frac{\sigma_0}{E}\right]^{\frac{1}{2}}$$

$$\gamma = \left[6\frac{E_0}{E}\frac{h}{h_0}\right]^{\frac{1}{2}}$$

Where G_0, E_0, E are the adhesive shear and Young's moduli and Young's modulus of the adherend respectively; h_0, h, are the respective thickness of the adhesive and adherend. $2c$—is the overlap length, ν—is Poisson's ratio of the adherend.

Acknowledgement

The authors are indebted to Mr. Y. Miller for his assistance in different parts of the work, and to Dr. J. Schmorak for his help in editing this paper.